

## Thermodynamics of SU(3) gauge theory at fixed lattice spacing

---

T. Umeda<sup>\*a</sup>, S. Ejiri<sup>b</sup>, S. Aoki<sup>a,c</sup>, T. Hatsuda<sup>d</sup>, K. Kanaya<sup>a</sup>, Y. Maezawa<sup>e</sup>, H. Ohno<sup>a</sup>  
(WHOT-QCD Collaboration)

<sup>a</sup> Graduate School of Pure and Applied Sciences, University of Tsukuba, Tsukuba, Ibaraki 305-8571, Japan

<sup>b</sup> Physics Department, Brookhaven National Laboratory, Upton, New York 11973, USA

<sup>c</sup> RIKEN BNL Research Center, Brookhaven National Laboratory, Upton, New York 11973, USA

<sup>d</sup> Department of Physics, The University of Tokyo, Tokyo 113-0033, Japan

<sup>e</sup> En'yo Radiation Laboratory, Nishina Accelerator Research Center, RIKEN, Wako, Saitama 351-0198, Japan

E-mail: tumeda@het.ph.tsukuba.ac.jp

We study thermodynamics of SU(3) gauge theory at fixed scales on the lattice, where we vary temperature by changing the temporal lattice size  $N_t = (Ta_t)^{-1}$ . In the fixed scale approach, finite temperature simulations are performed on common lattice spacings and spatial volumes. Consequently, we can isolate thermal effects in observables from other uncertainties, such as lattice artifact, renormalization factor, and spatial volume effect. Furthermore, in the EOS calculations, the fixed scale approach is able to reduce computational costs for zero temperature subtraction and parameter search to find lines of constant physics, which are demanding in full QCD simulations. As a test of the approach, we study the thermodynamics of the SU(3) gauge theory on isotropic and anisotropic lattices. In addition to the equation of state, we calculate the critical temperature and the static quark free energy at a fixed scale.

*The XXVI International Symposium on Lattice Field Theory*  
July 14-19 2008  
Williamsburg, Virginia, USA

---

\*Speaker.

## 1. Introduction

Since finite temperature ( $T > 0$ ) lattice QCD is performed on lattice with a temporal extent  $N_t = 1/aT$ , qualitative calculations at high  $T$  may require lower simulation cost than that at  $T = 0$ . However quantitative systematic studies at  $T > 0$  need huge simulation cost often more than that at  $T = 0$ . Because such study requires  $T = 0$  calculations at wide range of lattice scale. It is a reason why recent large scale thermodynamics calculations are often performed with the Staggered type quark formulations [1], which needs lower computational cost than that with Wilson type formulations [3], the domain wall and overlap quarks are all the more costly. To make matters worse, some Wilson type quarks sometimes cause some problems at coarse lattice, e.g. nonperturbative clover coefficient  $c_{SW}$  is reliably determined at  $a \sim 0.1$  fm or finer [4], and the domain wall quarks encounter with strong residual quark mass effects at coarse lattice [5]. In spite of the difficulties, results at  $T > 0$  with the Wilson type quark formulations are desired, because the Staggered type quarks suffer from problems of the flavor symmetry violation and the rooted Dirac operators.

Therefore we propose an alternative fixed scale approach to study thermodynamics of QCD, where we vary  $T$  by varying the temporal lattice size  $N_t = (Ta_t)^{-1}$  instead of the conventional fixed  $N_t$  approach. In the fixed scale approach,  $T = 0$  results are common for each  $N_t$  ( $T$ ) simulations. It may be able to reduce total simulation cost drastically. Furthermore, common parameters (except for  $N_t$ ) enable us to investigate pure thermal effects of observables without obstacles coming from changing lattice spacing and spatial volume effects.

In this report, we test the approach in the  $SU(3)$  gauge theory on isotropic and anisotropic lattices. Our lattice action and some details of the EOS calculation are given in Sect.2.1 and Sect.2.2. Results of EOS are presented in Sects.2.3 and 2.4. The  $T_c$  and the static quark free energy are discussed in Sect.3 and 4. We conclude in the last section.

## 2. Equation of state

### 2.1 T-integration method

In the fixed scale approach, to calculate the pressure non-perturbatively, we propose a new method, “the T-integral method” [6] :

$$\frac{p}{T^4} = \int_{T_0}^T dT \frac{\varepsilon - 3p}{T^5} \quad (2.1)$$

based on another thermodynamic relation valid at vanishing chemical potential:

$$T \frac{\partial}{\partial T} \left( \frac{p}{T^4} \right) = \frac{\varepsilon - 3p}{T^4}. \quad (2.2)$$

The initial temperature  $T_0$  is chosen such that  $p(T_0) \approx 0$ . Calculation of  $\varepsilon - 3p$  requires the beta functions just at the simulation point, but no further Karsch coefficients are necessary. Since  $T$  is restricted to have discrete values, we need to make an interpolation of  $(\varepsilon - 3p)/T^4$  with respect to  $T$ .

Since the coupling parameters are common to all temperatures, our fixed scale approach with the  $T$ -integral method has several advantages over the conventional approach; (i)  $T = 0$  subtractions

can be done by a common  $T = 0$  simulation, (ii) the condition to follow the LCP is obviously satisfied, and (iii) the lattice scale as well as beta functions are required only at the simulation point. As a result of these, the computational cost needed for  $T = 0$  simulations is reduced drastically.

When we adopt coupling parameters from  $T = 0$  spectrum studies, the values of  $N_t$  around and below the critical temperature  $T_c$  are much larger than those used in conventional fixed  $N_t$  studies. For example, at  $a \approx 0.07$  fm,  $T \sim 175$  MeV is achieved by  $N_t \sim 16$ . Therefore, for thermodynamic quantities around and below  $T_c$ , we can largely reduce the lattice artifacts over the conventional approach, with much smaller total computational cost. This is also a good news for phenomenological applications of the EOS, since the temperature achieved in the relativistic heavy ion collision at RHIC and LHC will be at most up to a few times the  $T_c$  [7]. We note here that, as  $T$  increases,  $N_t$  becomes small and hence the lattice artifact increases. Therefore, our approach is not suitable for studying how the EOS approaches the Stephan-Boltzmann value in the high  $T$  limit.

## 2.2 Lattice action

We study the  $SU(3)$  gauge theory with the standard plaquette gauge action on an anisotropic lattice with the spatial (temporal) lattice size and scale  $N_s$  ( $N_t$ ) and  $a_s$  ( $a_t$ ), respectively. The lattice action is given by

$$S = \beta \xi_0 \sum_x \sum_{i=1}^3 \left[ 1 - \frac{1}{3} \text{ReTr} U_{i4}(x) \right] + \frac{\beta}{\xi_0} \sum_x \sum_{i>j=1}^3 \left[ 1 - \frac{1}{3} \text{ReTr} U_{ij}(x) \right] \quad (2.3)$$

$$\stackrel{\text{def.}}{=} 3N_s^3 N_t \beta (\xi_0 P_t + \xi_0^{-1} P_s) \quad (2.4)$$

where  $U_{\mu\nu}(x)$  is the plaquette in the  $\mu\nu$  plane and  $\beta$  and  $\xi_0$  are the bare lattice gauge coupling and bare anisotropy parameters. The trace anomaly is calculated by

$$\frac{\varepsilon - 3p}{T^4} = \frac{N_t^3}{N_s^3 \xi^3} a_s \left( \frac{\partial \beta}{\partial a_s} \right)_\xi \left\langle \left( \frac{\partial S}{\partial \beta} \right)_\xi \right\rangle \quad (2.5)$$

$$= \frac{3N_t^4}{\xi^3} \left\langle \left( a_s \frac{\partial \beta}{\partial a_s} \right)_\xi \left[ \left\{ \frac{1}{\xi_0} P_s + \xi_0 P_t \right\} - \frac{\beta}{\xi_0} \left( \frac{\partial \xi_0}{\partial \beta} \right)_\xi \left\{ \frac{1}{\xi_0} P_s - \xi_0 P_t \right\} \right] \right\rangle \quad (2.6)$$

with  $\xi = a_s/a_t$  the renormalized anisotropy.  $a_s(\partial\beta/\partial a_s)$  is the beta function.  $\partial\xi_0/\partial\beta$  vanishes on isotropic lattices.

## 2.3 EOS on isotropic lattice

Our simulation parameters are listed in Table 1. On isotropic lattices, we calculate EOS on three lattices to study the volume and lattice spacing dependences. The ranges of  $N_t$  correspond to  $T = 210\text{--}700$  MeV for the sets i1 and i2, and  $T = 220\text{--}730$  MeV for i3, to be compared with  $T_c \sim 290$  MeV. The set a2 will be discussed later. The  $T = 0$  subtraction is performed with  $N_t = 16$  for i1 and i2, and with  $N_t = 22$  for i3. We generate up to a few millions configurations using the pseudo-heat-bath algorithm. Statistical errors are estimated by the Jackknife analysis. appropriate bin sizes, which strongly depend on  $T$ . Typically, bin size of a few thousands configurations are necessary near  $T_c$ , while a few hundreds are sufficient off the transition region.

| set | $\beta$ | $\xi$ | $N_s$ | $N_t$ | $r_0/a_s$            | $a_s$ [fm] | $L$ [fm] | $a(dg^{-2}/da)$ |
|-----|---------|-------|-------|-------|----------------------|------------|----------|-----------------|
| i1  | 6.0     | 1     | 16    | 3-10  | $5.35^{(+2)}_{(-3)}$ | 0.093      | 1.5      | -0.098172       |
| i2  | 6.0     | 1     | 24    | 3-10  | $5.35^{(+2)}_{(-3)}$ | 0.093      | 2.2      | -0.098172       |
| i3  | 6.2     | 1     | 22    | 4-13  | 7.37(3)              | 0.068      | 1.5      | -0.112127       |
| a2  | 6.1     | 4     | 20    | 8-34  | 5.140(32)            | 0.097      | 1.9      | -0.10704        |

**Table 1:** Simulation parameters on isotropic and anisotropic lattices. On isotropic lattices, we adopt  $r_0/a$  of [8], and the beta function of [9]. Anisotropic  $r_0/a_s$  is from [10], and the beta function is calculated in [6]. Lattice scale  $a_s$  and lattice size  $L = N_s a_s$  are calculated with  $r_0 = 0.5$  fm.

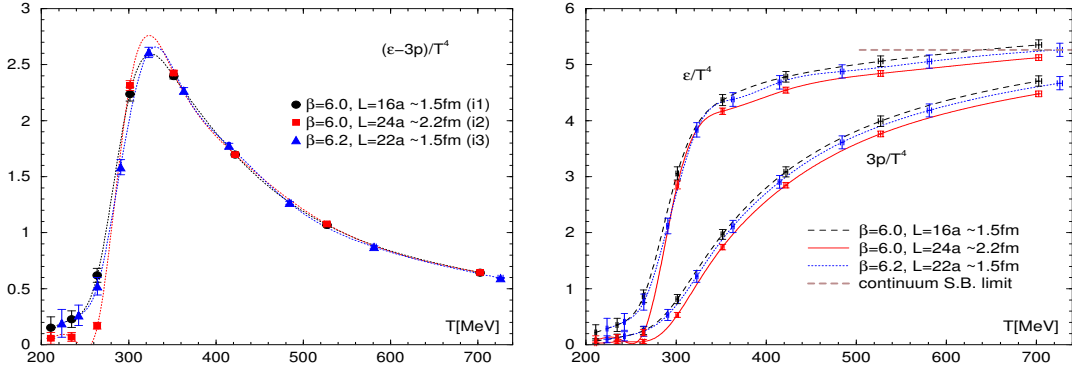


**Figure 1:** (Left) Trace anomaly on isotropic lattices. The dotted lines are natural cubic spline interpolations. Horizontal errors due to the lattice scale are smaller than the symbols. (Right) The energy density and the pressure on isotropic lattices.

Figure 1 (Left) shows  $(\varepsilon - 3p)/T^4$ . Dotted lines in the figure are the natural cubic spline interpolations. At and below  $T_c$ , lattice size dependence is visible between the sets i1 ( $L \approx 1.5$  fm) and i2 (2.2 fm). On the other hand, the lattice spacing dependence is small between i1 ( $a \approx 0.093$  fm) and i3 (0.068 fm). At higher  $T$ ,  $(\varepsilon - 3p)/T^4$  on three lattices show good agreement. The integration of (2.1) is performed numerically using the natural spline interpolations shown in Fig.1 (Left). For the initial temperature  $T_0$  of the integration, we linearly extrapolate the  $(\varepsilon - 3p)/T^4$  data at a few lowest  $T$ 's because the values of  $(\varepsilon - 3p)/T^4$  at our lowest  $T$  are not exactly zero. In this study, we commonly take  $T_0 = 150$  MeV as the initial temperature which satisfies  $(\varepsilon - 3p)/T^4 = 0$ , and estimate the integration from  $T_0$  to the lowest  $T$  by the area of the triangle. Statistical errors for the results of integration are estimated by a Jackknife analysis [11]. Note that the error in the lattice scale do not affect the dimension less quantity  $p/T^4$ .

In Fig.1 (Right), we summarize the results of EOS on isotropic lattices.  $\varepsilon/T^4$  is calculated combining the results of  $p/T^4$  and  $(\varepsilon - 3p)/T^4$ . Since the lattice parameter dependence of  $(\varepsilon - 3p)/T^4$  is small except for the vicinity of  $T_c$ , we find that EOS has a similar shape except for the vicinity of  $T_c$ . Near and below  $T_c$ , we observe a sizable finite volume effect between  $L \approx 1.5$  fm and 2.2 fm, while the lattice spacing effects are not so. At large  $T$ , we note a slight tendency that  $p$  and  $\varepsilon$  decrease as the lattice size becomes larger and the lattice spacing becomes smaller. Our results are qualitatively consistent with the previous results by the conventional fixed  $N_t$  method

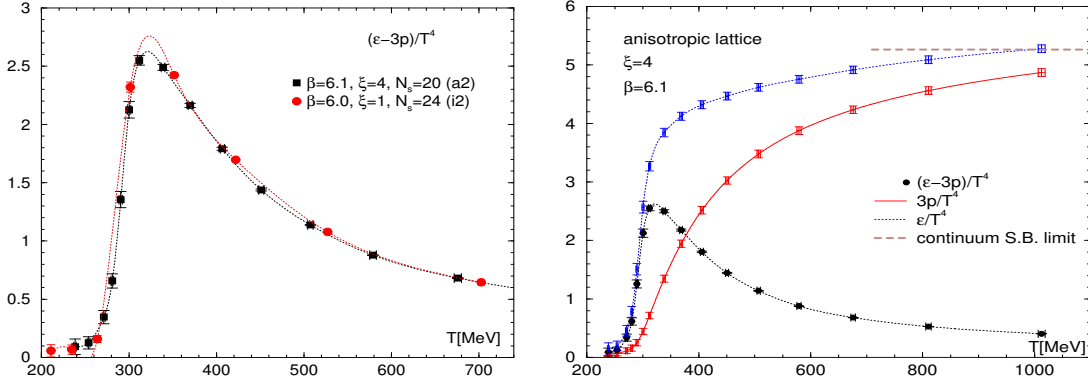


**Figure 2:** (Left) The trace anomaly on the anisotropic lattice (a2) and the isotropic lattice (i2). Dotted lines show the cubic spline interpolation. (Right) The EOS on the anisotropic lattice.

[9], but with much reduced lattice artifacts around  $T_c$  due to much larger  $N_t$  there.

## 2.4 EOS on anisotropic lattice

The anisotropic lattice with the temporal lattice finer than the spatial one is expected to improve the resolution of  $T$  without much increasing the computational cost. To further test the systematic error due to the resolution of  $T$ , we perform the study with the  $T$ -integral method on an anisotropic lattice with the renormalized anisotropy  $\xi = 4$ . The simulation parameters are given as the set a2 in Table 1, which are the same as those adopted in [10]. We vary  $N_t = 34-8$  corresponding to  $T = 240-1010$  MeV. The  $T = 0$  subtraction is performed with  $N_t = 80$ . We generate up to a few millions configurations. The beta function  $a_s(\partial\beta/\partial a_s)_\xi$  with  $\xi = 4$  has calculated in our paper [6], and its value at our simulation point is given in Table 1. For  $(\partial\xi_0/\partial\beta)_\xi$  we adopt the result of [12].

In Fig. 2 (Left), we compare the trace anomaly obtained on the anisotropic lattice with that on the isotropic lattice with similar  $a_s$  and  $L$  (the set i2). We find that the results are generally consistent with each other except for around  $T_c$ . We note a systematic tendency that the trace anomaly on the anisotropic lattice is slightly lower than that on the isotropic lattice. According to this tendency, the pressure on the anisotropic lattice is slightly smaller than that on the isotropic lattice at high  $T$ . The tendency may be understood by the smaller lattice artifact due to the temporal lattice spacing on anisotropic lattices, since lattice artifacts due to temporal lattice spacing are larger than that by the spatial lattice spacings in thermodynamic quantities [13]. Finally, we summarize our results of EOS on the anisotropic lattice in Fig. 2 (Right). We find that they are consistent with those on isotropic lattices.

## 3. Transition temperature

Here we consider a possibility to compute the  $T_c$  in the fixed scale approach.  $T_c$  is determined by studying temperature dependence of order parameters. Strictly speaking, such temperature dependence should be separated from other effects, such as renormalization, lattice artifacts, and spatial volume dependence. In the fixed scale approach, we can easily isolate the thermal effect on the observables. On the other hand, the resolution of  $T$  is restricted by discrete  $N_t$ .

| set  | $\beta$ | $\xi$ | $N_s$ | $N_t$ | $r_0/a_s$ | $a_s[\text{fm}]$ | $L[\text{fm}]$ |
|------|---------|-------|-------|-------|-----------|------------------|----------------|
| a2-1 | 6.1     | 4     | 20    | 26-30 | 5.140(32) | 0.097            | 1.9            |
| a2-2 | 6.1     | 4     | 30    | 26-30 | 5.140(32) | 0.097            | 2.9            |
| a2-3 | 6.1     | 4     | 40    | 26-30 | 5.140(32) | 0.097            | 3.9            |

**Table 2:** Simulation parameters on anisotropic lattices to study volume dependence of the susceptibility of the Polyakov loop.

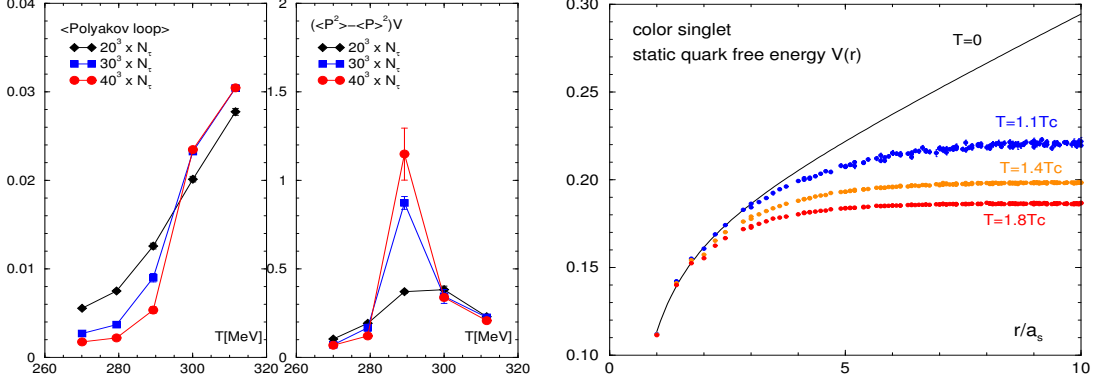


**Figure 3:** (Left,Center) Polyakov loop and its susceptibility on the anisotropic lattice. (Right) Static quark free energy on the anisotropic lattice.

We calculate the Polyakov loop and its susceptibility on the anisotropic lattice. In addition to the lattices prepared for the EOS calculation, we generated different spatial volume lattices to study its finite size scaling. The parameters we adopted are listed in Table 2. Since the  $SU(3)$  gauge theory has the global  $Z(3)$  symmetry, we calculate the real part of  $Z(3)$ -rotated Polyakov loop and its susceptibility. Our results are shown in the left and center panels of Fig.3. Unlike the case of conventional fixed  $N_t$  studies, the renormalization factor is common to all temperatures. From the susceptibility data we can find that the transition point locates at  $N_t \approx 28$  corresponds to  $T_c = 280$ - $300$  MeV from the  $r_0$  scale setting. We also find that the peak height of the susceptibility increases with increasing the system volume, in accordance with the 1st order nature of the transition.

#### 4. Static quark free energy

Finally, we study the static quark free energy  $V(r)$  in the fixed scale approach. In conventional fixed  $N_t$  studies, the additive renormalization constant for  $V(r)$  is different for each  $T$  because the lattice spacing is different. Assuming that the short distance physics is independent of  $T$ , the constant term is conventionally adjusted by hand such that  $V(r)$  around the smallest  $r$  coincide with each other.

In the fixed scale approach, on the other hand, the common lattice spacing for all  $T$  implies that the constant term in  $V(r)$  should be common too. Therefore, we can purely study the  $T$  effects without adjusting the constant term. In Fig.3 (Right) we show our results of  $V(r)$  for the color singlet channel on the anisotropic lattice, without adjusting the constant term. The solid curve in

the figure is a fit result of  $T = 0$  potential. We find that  $V(r)$  at different temperatures converge to a common curve at short distances. We thus have confirmed the expectation that the short distance physics is independent of  $T$ .

## 5. Conclusions

We proposed a fixed scale approach to study the QCD thermodynamics on the lattice. In this approach,  $T$  is varied by changing the temporal lattice size  $N_t$  at a fixed lattice scale. To test the method, we applied it to the  $SU(3)$  gauge theory on isotropic and anisotropic lattices. We found that the  $T$ -integral method to calculate the EOS works quite well. The main advantage of our approach is that the computational cost for  $T = 0$  simulations, which are the most time consuming calculations in the conventional fixed  $N_t$  approaches, can be drastically reduced. We may even borrow configurations of existing high precision simulations at  $T = 0$ . The approach is applicable to QCD with dynamical quarks too. We are currently investigating EOS in  $2 + 1$  flavor QCD with non-perturbatively improved Wilson quarks, using the configurations by the CP-PACS/JLQCD Collaboration [14]. With these fine lattices, the lattice artifacts around  $T_c$  are much smaller than the conventional fixed  $N_t$  approaches. We are further planning to use the PACS-CS configurations just at the physical point [15].

TU thanks H. Matusufuru for helpful discussions and comments. The simulations have been performed on supercomputers at RCNP, Osaka University and YITP, Kyoto University. This work is in part supported by Grants-in-Aid of the Japanese Ministry of Education, Culture, Sports, Science and Technology (Nos. 17340066, 18540253, 19549001, and 20340047). SE is supported by U.S. Department of Energy (DE-AC02-98CH10886).

## References

- [1] C. DeTar, plenary talk at LATTICE 2008, to be published in PoS (LATTICE2008) 001.
- [2] J. Engels, J. Fingberg, F. Karsch, D. Miller and M. Weber, Phys. Lett. B **252**, 625 (1990).
- [3] A. Ali Khan *et al.* [CP-PACS collaboration], Phys. Rev. D **64**, 074510 (2001).
- [4] S. Aoki *et al.* [CP-PACS Collaboration and JLQCD Collaboration], Phys. Rev. D **73**, 034501 (2006).
- [5] P. Chen *et al.*, Phys. Rev. D **64**, 014503 (2001).
- [6] T. Umeda *et al.* [WHOT-QCD collaboration], arXiv:0809.2842 [hep-lat].
- [7] T. Hirano, N. van der Kolk and A. Bilandzic, arXiv:0808.2684 [nucl-th].
- [8] R. G. Edwards, U. M. Heller and T. R. Klassen, Nucl. Phys. B **517**, 377 (1998).
- [9] G. Boyd *et al.*, Nucl. Phys. B **469**, 419 (1996).
- [10] H. Matusufuru, T. Onogi and T. Umeda, Phys. Rev. D **64**, 114503 (2001).
- [11] M. Okamoto *et al.* [CP-PACS Collaboration], Phys. Rev. D **60**, 094510 (1999).
- [12] T. R. Klassen, Nucl. Phys. B **533**, 557 (1998).
- [13] Y. Namekawa *et al.* [CP-PACS Collaboration], Phys. Rev. D **64**, 074507 (2001).
- [14] T. Ishikawa *et al.* [JLQCD Collaboration], Phys. Rev. D **78**, 011502 (2008).
- [15] Y. Kuramashi, plenary talk at LATTICE 2008, to be published in PoS (LATTICE2008) 018.